



Title	Classification of sound-scattering layers using swimming speed estimated by acoustic Doppler current profiler
Author(s)	Lee, Kyounghoon; Mukai, Tohru; Lee, Dae-Jae; Iida, Kohji
Citation	Fisheries science, 80(1), 1-11 https://doi.org/10.1007/s12562-013-0683-9
Issue Date	2014-01
Doc URL	http://hdl.handle.net/2115/57396
Rights	The original publication is available at www.springerlink.com
Type	article (author version)
File Information	20131024FishSci_KLEEetal.pdf



[Instructions for use](#)

Title:

Classification of sound scattering layers using swimming speed estimated by acoustic Doppler current profiler

Running Title:

Classification of SSL by ADCP

Authors and their affiliations:

KYOUNGHOON LEE¹, TOHRU MUKAI^{2*}, DAE-JAE LEE³ AND KOHJI IIDA²

¹Fisheries System Engineering Division, National Fisheries Research & Development Institute, Busan, 619-705, KOREA

²Laboratory of Marine Environment & Resource Sensing, Faculty of Fisheries Sciences, Hokkaido University, Hakodate, Hokkaido, 041-8611, JAPAN

³Division of Marine Production System Management, Pukyong National University, Busan, 608-737, KOREA

^{2*} Corresponding author:

Tel: 81-138-40-8853. Fax: 81-138-40-8854.

E-mail: mukai@fish.hokudai.ac.jp

Abstract

There are various techniques for identifying fish species, such as the multi-frequency method, *in situ* target strength characteristics, and digital image processing methods. Acoustic Doppler current profilers (ADCPs) are able to simultaneously determine multiple current fields and have been used to observe the swimming speed and behavior patterns of shoals of pelagic fish under natural conditions. In this study, we evaluated a classification method that determined the swimming velocity of the sound scattering layer as well as pelagic fish shoals using ADCP (153.6 kHz) and a scientific echo sounder (38, 200 kHz). To calculate the actual swimming speed, the mean swimming velocity vectors of each stratified bin must be compared with the mean surrounding 3-D current velocity vectors. The average 3-D swimming velocity of the sound scattering layer was found to be characterized by a deviation of >5.3 cm/s from the surrounding current field. The average 3-D swimming velocity of Pacific saury *Cololabis saira* was calculated as 91.3 cm/s, while that of lanternfish *Diaphus theta* was 28.1 cm/s. These swimming speeds corresponded to 4.19 and 4.26 times the body length (BL/s), respectively. Thus, use of ADCP swimming velocity data is expected to be a valuable species identification method for various fishes distributed in the survey area.

Keywords: acoustic Doppler current profiler, sound scattering layer, Pacific saury, lanternfish, swimming velocity, 3-D velocity vector

INTRODUCTION

When estimating the density distribution and abundance of scatter objects in the water using acoustic techniques, identifying the species of the specific scatterer is important. The sound scattering layer comprises various zooplankton and nekton mixed with fish predating on them at night; thus, it is very difficult to discriminate among species in the sound scattering layer. The two-frequency difference method developed recently can separate shoals of fish and zooplankton based on differences between their target strength using low and high frequency characteristics simultaneously in an acoustical scattering theoretical model [1–3].

Acoustic Doppler current profilers (ADCPs) have frequently been used on survey vessels and fishing boats to measure current speed and direction, manage fishing gear, and obtain information on fisheries. ADCPs are now able to measure current fields over the entire water column and identify the density distribution and behavior of zooplankton in the sound scattering layer. For pelagic fish species, swimming speed has been measured by Doppler sonar using the Doppler shift associated with swimming patterns [4, 5].

Behavioral pattern analysis using an ADCP equipped on a survey vessel has shown advantages in determining the speed of migration of pelagic fish in natural environments [6, 7]. This method has the disadvantage that it can only be applied to a school of fish in which the scatterers are distributed widely within the water column and are simultaneously contacted by several beams emitted by the ADCP to measure the current field. In addition, post-processing of the acquired data due to rolling and pitching of the vessel is required. Multi-frequency scientific echo sounders with high resolution have been applied to measure the swimming speed of a school of fish through single fish

detection algorithms for estimating the distribution and density of a school of fish [8, 9]. Although single fish detection algorithms are advantageous in identifying both the swimming speed and swimming tilt angles of individuals, they are not applicable to a school of fish with a larger population density, in contrast to ADCP.

Thus, ADCP is able to measure the migration patterns of zooplankton making up a sound scattering layer and swimming behavior and speed of a school of fish simultaneously. Measurement of the migration speed of a specific school of fish provides valuable data on behavior patterns and for operation of fishing gear. In addition, using 3-dimensional (3-D) swimming velocity vectors, it is possible to estimate the pitch angle primarily affecting the density distribution of a school of fish [6, 7, 10].

In this study, migration patterns of a sound scattering layer along sea currents in Funka Bay off the east coast of Oshima Peninsula, northern Japan, and surroundings and the migration speed of a school of fish within the layer were measured using ADCP. Based on the mean volume backscattering strength calculated from the echo intensity by the ADCP, 3-D swimming velocity vectors were used to differentiate a school of fish from the general sound scattering layer, suggesting a method for species identification of fish and zooplankton.

MATERIALS AND METHODS

Survey area and sampling

This study targeted the sound scattering layer distributed offshore of Funka Bay in September 2003. Acoustical data were obtained with an ADCP (Ocean Surveyor 153.6kHz, RD-Instruments, USA) and a scientific echosounder (ER-60, SIMRAD,

Norway) at frequencies of 38 and 200 kHz. Biological sampling was conducted by towing a Frame-type Midwater Trawl (2 m × 2 m) net at 3 – 4 knots to identify the distribution of small fish and nekton present in the sound scattering layer, however a shoal of large fish, which is distributed in the surface area, could be caught as well as those of small fish by the sampling gear in the survey. After the samples were collected, acoustical data were gathered to measure the swimming speed of each school of fish with the survey vessel drifting in a nearby survey area.

Algorithm for estimating the speed of a school of fish

An algorithm for excluding data associated with fish can be developed by controlling the system file (CF command file) when the data are collected. Raw data are collected at 1- or 2-min intervals. The fish rejection algorithm is then determined by the value of “percent good” (the percentage of pings that pass the data rejection criteria), and if the level determined by the 4 beams is greater than the ADCP threshold applied in the averaging process, the bin is removed. Using the average of all of the collected data, the presence of an echo signal can be identified. Therefore, by using the raw data rather than the averaged data, the speed associated with the fish can be estimated in reverse. RDI, the manufacturer of the ADCP, compared the echo signal of each beam used for averaging, and the ADCP was set not to average data greater than a threshold level designated in the command file (Table 1).

A fish rejection algorithm suggested by Plimpton *et al.* [11] was considered to obtain marine environmental parameters. If the echo intensity value of at least one beam is greater than the others, the current vector associated with a school of fish is included in the current field data. In that case, the current vector of that bin is not used for averaging

and the echo intensity immediately below the bin is selected. It is possible to estimate the migration speed when there is a clear echo signal in the volume backscattering strength produced by a school of fish within the beams of ADCP. For an ADCP consisting of 4 beams, raw data for analysis should include at least 3 beams and averaged data should use all 4 beams [6]. Therefore, the fish rejection algorithm applied to the ADCP data removes the current vector of the bin when it is determined that it contains errors in velocity, i.e., if 1) the echo intensity of a bin is too large for each beam of an ADCP due to scattering by a school of fish or 2) differences in echo intensity received by the 4 beams are relatively large. By clearing the function of the fish rejection algorithm, the swimming speed of a targeted school of fish having a wide spatial distribution can be estimated. To estimate the migration speed of a school of Pacific saury, the fish rejection algorithm was removed as suggested by Demer *et al.* [6] and the data were recorded as shown in Table 1 and Fig. 1.

Calculating the volume backscattering strength of the integrated bin

A vessel-mounted ADCP on the T/S Ushio Maru of Hokkaido University was used for the survey. It consisted of 4 beams with a frequency of 153.6 kHz and the angle of the beam with respect to vertical was 30°. Data were collected with a pulse interval of 1 s; the thickness of the bin was 4 m and the averaging time was 30 s. The collected echo intensity data during the survey period were used to determine the average echo intensity for the bins at each water depth for each beam. The volume backscattering strength (dB re 1 m⁻³, *SV*) was calculated using the following equation (1) [12]:

$$SV = C + 10\log_{10}\left((T_x + 273.16)R^2\right) - L_{DBM} - P_{DBW} + 2\alpha r + K_c(E - E_r) \quad (1)$$

where C is a constant (-143.5 dB), T_X is the internal temperature of the transducer ($^{\circ}\text{C}$), R is the slant range to the scatterers (m), P_{DBW} is the transmitting power (Watts), α is the absorption coefficient (0.053 at 15.4 $^{\circ}\text{C}$, 33.8 PSU, and 153.6 kHz to 50 m depth), and E_r is the received noise level (counts), L_{DBM} is $10\log_{10}(\text{transmit pulse length, m})$, K_C is RSSI scale factor (dB/count), E is echo strength (RSSI, counts).

Fish swimming speed

The standard deviation of horizontal velocity (SD_{HV}) of the broadband ADCP measurements collected in this study was calculated using the following equation [13, 14]:

$$SD_{HV} = \frac{1.5V_a}{\pi} \left[\frac{(R_{TL}^{-2} - 1) \cdot 2 \cdot c \cdot \cos \theta}{f_0 D N} \right]^{1/2} \quad (2)$$

where f_0 is the transmitting frequency (Hz), D is the depth cell length of the bin (m), N is the mean number of pings (count), V_a is the ambiguity velocity (m/s), R_{TL} is the timelag correlation of the trans-receiving signals, c is the speed of sound (m/s), and θ is the beam tilt angle from vertical. For the broadband ADCP used in this study, D , C , V_a , and R_{TL} were set to 4 m, 1,507 m/s, 33 cm/s, and 0.5, respectively; thus, the resolution obtained was approximately 1.8 cm/s. When the horizontal current speed was measured, there were deviations in the current field from swimming marine organisms; therefore, the current field was examined when the sound scattering layer migrated downward to ~80 m depth after sunrise. In addition, the migration speed of a school of fish was estimated when the backscattering strength (SV) of the bin had an echo intensity ≥ -70 dB over 0 – 50 m depth. The data were used to calculate the horizontal current field with

an east–west current vector (V_{EW}) and a north-south current vector (V_{NS}) averaged over 30-s intervals as shown in equations (3) and (4) below:

$$\pm \bar{V}_{EW} = \frac{\sum_{n=1}^N V_{EWn}}{N} , \quad \pm \bar{V}_{NS} = \frac{\sum_{n=1}^N V_{NSn}}{N} \quad (3)$$

$$\bar{V}_H = \sqrt{\bar{V}_{EW}^2 + \bar{V}_{NS}^2} \quad (4)$$

Herein, (+) and (-) values represent that East and North directions are positive while West and South are negative vectors, respectively.

The mean horizontal swimming speed (\bar{V}_{Hf}) of a school of fish in an average current field in a nearby water zone can be calculated using equation (5), in which f and w represent a school of fish and the horizontal current field in the nearby water zone, respectively. Thus, \bar{V}_{Hf} of a school of fish relative to the mean horizontal current field is calculated as follows:

$$\bar{V}_{Hf} = \sqrt{(\bar{V}_{EWf} - \bar{V}_{EWw})^2 + (\bar{V}_{NSf} - \bar{V}_{NSw})^2} \quad (5)$$

The ADCP is able to measure the horizontal current vector (V_H) and the vertical current vector (V_v), allowing estimation of the 3-D swimming speed vector (V_{3D}) of a school of fish. Therefore, the 3-D swimming speed and swimming tilt angle (ϕ_{3D}) estimated from the 3-D speed including the vertical swimming direction can be determined using the following equations:

$$\bar{V}_{3D} = \sqrt{\bar{V}_{Hf}^2 + \bar{V}_{vf}^2} \quad (6)$$

$$\phi_{3D} = \begin{cases} \arctan(V_{vf} / V_{Hf}) & (\text{if } V_{vf} \geq 0 \text{ and } V_{Hf} \geq 0) \\ \arctan(V_{Hf} / V_{vf}) - 90^\circ & (\text{if } V_{vf} < 0 \text{ and } V_{Hf} < 0) \\ -(\arctan(V_{Hf} / V_{vf}) + 90^\circ) & (\text{if } V_{vf} < 0 \text{ and } V_{Hf} \geq 0) \\ -\arctan(V_{vf} / V_{Hf}) & (\text{if } V_{vf} \geq 0 \text{ and } V_{Hf} < 0) \end{cases} \quad (7)$$

RESULTS

The survey vessel departed from Usujiri port in the southeast portion of the study area and measured the current field 20 m below the water surface until reaching St. 603 (42.00° N, 141.20° E). The measured current field is shown in Fig. 2. Throughout the study area, the current in the surface layer flowed southeastwards and that in the subsurface layer to 100 m depth flowed northwestwards. Echo intensity, vertical velocity, and the horizontal current field measured by the ADCP to 250 m below the water surface are shown in Fig. 3.

The properties of the current field, including water temperature and salinity distributions in the survey area, are shown in Fig. 3. The sound scattering layer, measured as the survey vessel transited, migrated upward at sunset (17:25) and was distributed within the surface and pelagic layers over a wide depth range. At all stations, the water temperature of the surface layer was 18 °C and it was stable at 12 °C until 70 m depth where fish schools were distributed. An intense pycnocline in the surface layer was observed due to the Tsugaru warm current, which has high temperature and salinity. In September in Funka Bay, the marine structure was complex due to the Tsugaru warm current and the low temperature–low salinity Kuril cold current producing maxima and minima, respectively, for water temperature and salinity within the vertical distributions. The Tsugaru warm current was present in the pelagic layer offshore of Funka Bay, moving northeastwards. Offshore of Funka Bay, the Oyashio cold current in the inshore water formed a southeastwards counterclockwise current field in the surface and sea bottom layers. The sound scattering layer had a strong current field moving toward the surface and the pelagic layer migrated upward, likely caused by scatterers having

swimming ability. Therefore, when the sound scattering layer migrated downward to 80 m water depth after sunrise, the resulting current field was compared with the actual current field in the sea nearby (Fig. 3).

The migration speed of the sound scattering layer was estimated based on an MVBS threshold of ≥ -80 dB from scatterers distributed to 100 m below the water surface at St. 603. In addition, using the measured east–west V_{EW} and north–south V_{NS} averaged over 30-s intervals, the current field was averaged by directional vector calculation, as shown in equation (4).

At St. 603, the average horizontal current speed (\bar{V}_H) was 19.6 cm/s and the average horizontal current direction ($\bar{\theta}$) was 328.1° N ($\bar{V}_{EW} = -10.34$ cm/s; $\bar{V}_{NS} = 16.59$ cm/s), consistent with the Tsugaru warm current. The sound scattering layer migrated up to the surface layer at sunset. The average horizontal swimming speed was 24.9 cm/s in the mean horizontal swimming direction. The mean swimming speed had a deviation of 7.0 cm/s and while migrating, had a direction consistent with the current direction in the adjacent sea.

Table 2 shows the species of zooplankton constituting the sound scattering layer that caused deviations in the current field from the mean. Based on the trawl samples from 20–50 m depth, the species comprising the sound scattering layer included euphausiids, copepods, amphipods, and chaetognaths. Among these species, euphausiids were most numerous at 82.8% with an average density of 73.7 ind/m^3 . The average body length of the euphausiids was 12.7 ± 1.11 mm with a maximum of 17.5 mm.

Swimming species of zooplankton found in the sound scattering layer included euphausiids, copepods, and amphipods. The primary species, euphausiids, were collected by net sampling and hence were considered to be the main scatterer causing

deviations in the horizontal current speed vectors in the sound scattering layer in the survey area.

Small numbers of Pacific saury were collected in Funka Bay while sampling for potential scatterers with a frame-type midwater trawl net in September 2003. During the experiment, a frame-type midwater trawl net was towed at 3–4 knots to identify zooplankton, such as nekton and euphausiids, distributed in the sound scattering layer outside of Funka Bay. When a school of Pacific saury appeared, 11 individuals of Pacific saury were collected in the samples. The averaged body length (\bar{L}) was 21.9 ± 4.0 cm.

The results of the calculations showed that the mean horizontal swimming speed (\bar{V}_{Hf}) of the school of Pacific saury was 72.4 cm/s and the mean horizontal swimming direction ($\bar{\theta}_{Hf}$) was 160.1° ($\bar{V}_{EWf} = 24.58$ cm/s; $\bar{V}_{NSf} = -68.08$ cm/s). At the same time, the mean swimming direction and the mean current direction were measured in the water layer in which the school of Pacific saury was present around the drifting survey vessel (Fig. 5).

The school of fish was migrating to the southeast, nearly opposite to the average current field ($\bar{\theta}_{Hw}$, 328.1° ; \bar{V}_{Hw} , 19.6 cm/s) at St. 603. Accordingly, the mean horizontal swimming speed (\bar{V}_{Hf}) of the school of fish relative to the mean horizontal current field was estimated as 88.6 cm/s.

The Pacific saury school observed with the ADCP was migrating southwards from Kuril current in the mid-fall along the southeast water zone near Hokkaido through Funka Bay towards the south–north water currents offshore of Japan.

The ADCP measures both the vertical current vector (\bar{V}_v) and the horizontal current

vector. Therefore, it is possible to estimate the 3-D migration velocity and the pitch angle of a swimming school of fish using a combination of the ADCP horizontal and vertical current vectors [6]. Using equation (6), the 3-D swimming velocity of the Pacific saury school was estimated as 91.3 cm/s. Using equation (7), the swimming pitch angle distribution was also estimated ($16.2^{\circ} \pm 12.4^{\circ}$) by calculating the 3-D vector velocity of each bin. The mean swimming velocity and mean swimming pitch angle with respect to the 3-D vector velocity were measured at night. Because Pacific saury are phototactic, the school of Pacific saury migrated along with the light of the vessel, which greatly affected the swimming velocity and the swimming pitch angle. The water temperature of the marine environment also affects the swimming ability of fish [15]. The water temperature of the vertical water column in which the fish were present (the surface layer, ~35 m) in this experiment was 14.1–17.6 °C. The optimum water temperature range for Pacific saury in the northeastern inshore water during the catch period (Sep. – Nov.) is 15–18 °C; thus, they were considered to be within their optimum temperature range.

Acoustic data were recorded by ADCP and a scientific echosounder on scatterers in the sound scattering layer distributed offshore of Funka Bay. Among the samples collected by the frame midwater trawl, lanternfish were found in November 2002 and Pacific saury were found in September 2003. Based on the schools of fish identified by ADCP, it was possible to distinguish the species of fish using swimming speed and environmental parameters such as distribution in the water column.

The swimming speed of lanternfish was determined by ADCP in the same manner as for Pacific saury. Figure 6 shows an echogram of the volume backscattering strength and current field distribution determined by the split beams (38, 200 kHz) of the scientific

echosounder during net sampling at St. 603. The threshold level was set to -70 dB. The echogram produced by the scientific echosounder indicated that a school of fish, distributed above and below 50 m depth at the time of net sampling, rose to 20 m, and as net sampling began, descended again and remained at 60 m depth. The ADCP echogram was averaged over 30-s intervals and recorded without removing the fish rejection algorithm during averaging. Accurate estimation of the mean horizontal swimming speed was not possible; however, the mean horizontal speed vector of the current field was located at a water depth where a school of fish was present, was faster than the current fields in nearby water layers, and arose from deviations in the velocity vector resulting from the school of fish. A downward velocity vector was found by measuring the vertical speed vector.

Therefore, to estimate the 3-D velocity vector of a school of fish, raw data rather than averaged data were used. In nearby water zones, characteristics of the current field were estimated by averaging bins with a threshold of ≤ -80 dB, which were not considered echo signals in the ADCP data averaged over 30-s intervals. Estimated values for the school of fish and the current field are shown in Fig. 7. Figure 7 (a) and (b) show the distribution of the mean horizontal swimming speed and direction of the school of fish, Figure 7 (c) shows the swimming pitch angle of the school of fish, Figure 7 (d) and (e) show the distributions of the two current fields, and Figure 7 (f) shows both length distributions of lanternfish collected by the trawl. The mean swimming speed of the lanternfish measured by ADCP was 23.0 ± 12.7 cm/s, the mean horizontal swimming direction was $164.4^\circ \pm 81.73^\circ$, and the swimming pitch angle distribution was $5.7^\circ \pm 26.1^\circ$. In addition, the horizontal swimming speed of the school of fish with respect to the current field in the nearby water zone (mean horizontal current speed, 8.0 cm/s;

mean horizontal current direction, 344.5°) was 28.0 cm/s. The 3-D mean swimming velocity was estimated at 28.1 cm/s by calculating the vertical velocity vector. However, the lanternfish collected from net sampling were divided into two length class distributions (longer, $n = 23$; shorter, $n = 33$). The maximum body length was 78.8 mm and the average body length (\bar{L}) was 35.7 mm. Individuals with longer body lengths, used for determining swimming velocity, had an average body length (\bar{L}) of 66.2 ± 6.1 mm.

DISCUSSION

A sound scattering layer distributed throughout the water column mainly consists of zooplankton and nekton. An ADCP measures the current field within the survey area associated with drifting scatterers present over a wide area of the sea. It cannot easily measure the velocities of swimmers; however, it can measure the vertical migration speed of a sound scattering layer causing deviations in the current field. The resolution of ADCP can be improved by averaging values measured over a long period, since averaging over a shorter period of time results in larger deviations in the sound scattering layer due to swimming species [16]. Contrasting ecological vs. physical oceanographic behaviors affecting the data, it is possible to estimate the swimming speed of a sound scattering layer with swimming species if the background current field is identified based on neighboring areas of the sea. The current meter is set up to measure discrete intervals and to estimate the characteristics of a current field based on comparison to current fields in nearby areas. The current field measured with an ADCP can be verified with a mechanical current meter (MCM). Plimpton *et al.* [11] used an MCM to verify deviations in the current field by investigating currents within the ADCP

survey area. At a certain water depth, use of an MCM to verify the reliability of ADCP measurements is necessary. However, when a survey vessel investigates a current field, considerable time is consumed in surveying, and therefore a bottom-mounted ADCP is used for comparison.

In this study, verification of the current field was required but a direct comparison was not performed. Because the current flow did not change quickly, verification of the current field was possible by comparing it to that in nearby areas [6]. Therefore, estimation of the current field in the sea was performed when the sound scattering layer moved downward at sunrise and remained at depth. The estimated current field in the same area of the sea was established as the absolute current value.

Because commercially available ADCP was not designed to measure the 3-D velocity of a school of fish, to minimize errors in measurement of the current field caused by different species of fish, a fish rejection algorithm was used that removes data representing the swimming speed of fish based on the sound scattering intensity determined by the maximum difference between the echo intensities of 4 beams.

The objective of this study was to estimate the migration speed of schools of fish residing in the inshore and offshore waters of Funka Bay, Hokkaido using ADCP data. The nearshore waters of Funka Bay are seasonally affected by the Kuril cold current from winter to summer and the high temperature and salinity of the Tsugaru warm current from summer to fall. Therefore, various species of pelagic fish are present seasonally.

Classification of fish species by acoustics can encounter many challenges that cannot be resolved by net sampling due to the differing characteristics of received echo intensities with various fish species and sizes. The target species are pelagic, which

swim in the pelagic layer. When estimating the swimming speed of a school of fish among many scatterers, quantitative ADCP data cannot be used in the bottom layer, because there are higher echo intensities and strong current fields due to measurement errors. Therefore, ADCP data can be only used in the whole water column excluding the surface layer and around the sea bottom.

The swimming speed of a fish is generally represented by a ratio, the speed divided by the body length. The average body length of the Pacific saury collected by net sampling was 21.9 cm, corresponding to 4.19 BL/sec 3-D mean swimming velocity. For lanternfish, the average body length of the larger body length distribution was 6.6 cm, corresponding to 4.26 BL/sec 3-D mean swimming velocity. For the demersal species above, swimming velocity relative to body length was faster than generally estimated for most demersal species; however, considering the differences between the estimated values, distinguishing between the species was possible. For future studies of demersal fish inhabiting specific waters, estimating swimming velocity could provide information allowing identification of species. Determining the pitch angle of a fish school using the 3-D velocity vector would allow better estimates of resource abundance.

ADCP measures the current field in the survey area by estimating the Doppler shift produced by scatterers, and estimates the current field by averaging and other arithmetical operations to improve accuracy. However, deviations in the current field caused by a migrating high-density school of fish distributed uniformly across the 4 beams could be removed by the suggested fish rejection algorithm. Conversely, by not applying this algorithm and receiving the Doppler shift uniformly, the 3-D swimming speed of a school of fish can be estimated by combination of the 4 beams. For a bin presumed to represent a school of fish based on an absolute threshold level, the

distribution of swimming pitch angles among all 4 beams in a bin was estimated by calculating vectors for horizontal and vertical swimming speed. As a result, for the phototactic Pacific saury, swimming velocity was determined to be higher than usual due to stimulation by the light from the vessel near the surface of the water at night. The measured distribution of swimming pitch angles tended to show upward migration.

For future studies, when the horizontal swimming speed of a school of fish is estimated using 4 beams and using raw data as suggested by Demer *et al.* [6], measured values for more than 3 beams ≤ 5 dB should be applied. In addition, the variation in mean volume backscattering strength relative to the direction of movement of a scatterer at each beam angle needs to be verified. Additionally, the swimming speed of Pacific saury in nature has not been confirmed. For small, demersal fish species in general, swimming speed is estimated to be 3 times the body length; however, there have been no studies of the swimming speed of Pacific saury in nature. Therefore, the swimming speed was estimated based on the body length of the Pacific saury determined from the net sampling data and the measured swimming speed.

Using the migration speed of a school of fish measured in nature, distinguishing demersal species inhabiting certain waters is possible by confirming the swimming speed using body lengths. When measuring velocities with ADCP, there is a defect (lower spatial resolution) preventing estimation of the target strength of each individual. This could be overcome by estimating the swimming speed of a fish based on body length, making identification of species possible. To estimate densities, variables affecting the target strength for an individual and the swimming tilt angle could be determined by calculating swimming tilt angles from the 3-D velocity vector. Therefore, application of ADCP may be of great benefit in estimating the biomass of living marine

resources.

ACKNOWLEDGEMENT

We thank the officers and crew of the T/S Ushio Maru, and thank Prof. Y. Fujimori for net sampling support. This study was partially supported by a Grant (RP-2013-FE-000) promoted by the National Fisheries Research and Development Institute of Korea, and also supported by the FiSCUP (Core University Program on Fisheries Science) between Pukyong National University and Hokkaido University funded by KRF and JSPS. Thanks are due to the editor and two anonymous reviewers for providing helpful comments.

REFERENCES

1. Madureira LSP, Everson I, Murphy EJ (1993) Interpretation of acoustic data at two frequencies to discriminate between Antarctic krill (*Euphausia superba* Dana) and other scatterers. J Plank Res 15:787–802
2. Miyashita K, Aoki I, Seno K, Taki K, (1997) Acoustic identification of isada Krill, *Euphausia pacifica* Hansen, off the Sanriku coast, north-eastern Japan. Fish Oceanogr 6:266–271.
3. Kang M, Furusawa M, Miyashita K (2002) Effective and accurate use of difference in mean volume backscattering strength to identify fish and plankton. ICES J Mar Sci 59:794–804

4. Holliday DV (1974) Doppler structure in echoes from schools of pelagic fish. *J Acoust Soc Am* 55:1313–1322
5. Zhou M, Nordhausen W, Huntley M (1994) ADCP measurements of the distribution and abundance of krills near the Antarctic Peninsula in water. *Deep-Sea Res* 41:1425–1445.
6. Demer DA, Barange M, Boyd AJ (2000) Measurements of three-dimensional fish school velocities with an acoustic Doppler current profiler. *Fish Res* 47:201–214
7. Zedel L, Knutsen T, Patro R (2003) Acoustic Doppler current profiler observations of herring movement. *ICES J Mar Sci* 60:846–859
8. Torgersen T, Kaartvedt S (2001) In situ swimming behavior of individual mesopelagic fish studied by split-beam echo target tracking. *ICES J Mar Sci* 53:346–354
9. Chu D, Jech JM, Lavery A (2003) Inference of geometrical and behavioral parameters of individual fish from echo-trace-analysis. *Deep-Sea Res I* 50:515–527
10. Lee KH, Lee DJ, Kim HS, Park SW (2010) Swimming speed measurement of Pacific saury (*Cololabis saira*) using acoustic Doppler current profiler. *J Kor Soc Fish Tech* 46:165–172
11. Plimpton PE, Freitag PH, McPhaden MJ (1997) ADCP velocity errors from pelagic fish schooling around equatorial moorings. *J Atmos Ocean Tech* 14:1212–1223
12. Deines KL (1999) Backscatter estimation using broadband acoustic Doppler current profilers. *Proceedings of the IEEE Sixth Working Conference on Current Measurement*, San Diego, USA
13. RD Instruments (1996a) *Acoustic Doppler Current Profiler, Principles of Operation a Practical Primer*. RD Instruments, San Diego, California, USA

14. RD Instruments (1996b) Field service technical paper 001 (FST-001) Broadband ADCP advanced principles of operation 01 October 1996. RD Instruments, San Diego, California, USA
15. Dickson KA, Donley JM, Sepulveda C, Bhoopat L (2002) Effect of temperature on sustained swimming performance and swimming kinematics of the chub mackerel *Scomber japonicus*. J Exp Biol 205:969–980
16. Wilson CD, Firing E (1992) Sunrise swimmers bias acoustic Doppler current profiles. Deep-sea Res, 39:885–892

Figure Legends & Tables

Fig. 1. Data processing to estimate the fish school's swimming speed by ADCP.

Fig. 2. Horizontal distribution current velocity along the track line of *T/S Ushio Maru* at a depth of 20 m measured by the shipboard ADCP offshore Funka Bay during September 27-28, 2003.

Fig. 3. Vertical distributions of MVBS, and current velocity along the tack line of *T/S Ushio Maru* measured by the shipboard ADCP. MVBS was averaged for one minute (a), and the current velocity displayed for vertical velocity component (+ : upward, - : downward) (b), horizontal velocity (c) and direction (d), respectively. Contour lines of temperature (c) and salinity (d) are superimposed on the chart.

Fig. 4. Distribution of horizontal moving velocity of Sound Scattering Layer (a, b) and horizontal current velocity of surrounding waters (c, d). The SSL was identified by the threshold of MVBS (> -80 dB).

Fig. 5. Distribution of swimming speed (a) and direction (b) of fish school and current speed of waters (c, d) estimated by ADCP. The echo from fish school was identified by the threshold level of MVBS (> -70 dB) and the noise margin less than 5 dB.

Fig. 6. Vertical distribution of MVBS and current velocity observed by scientific echo sounder and ADCP. The upper two echograms were obtained by 38 kHz and 200 kHz of EK60, and the lower four figures were obtained by MVBS, horizontal speed, horizontal direction, and vertical velocity from ADCP, respectively. Black line in the figure shows the track of Framed Midwater Trawl.

Fig. 7. Histograms of horizontal swimming speed (a), direction (b) and swimming angle (c) for lanternfish, and the current speed (d) and direction (e) of surrounding waters. Histogram of body length (f) of samples shows bimodal distribution. The large mode of body length was 66.2 mm (SD ; 6.1 mm).

Table 1. Command settings to configure the broadband ADCP (referred to Demer et al., 2000)

WS400	Depth cell size; set to 4 m
WF400	Blank after transmit; set to 4 m
WN120	Number of depth cells; set to 120
WP00001	Pings per ensemble; set to 1
WM1	Water profiling mode; set to 1
WA255	False-target threshold maximum; disabled with setting of 255
TP000100	Time between ping groups; set to 1s
EP0000	Pitch (tilt 1); set to 0.000 deg.
ER0000	Roll (tilt 2); set to 0.000 deg.
EZ1020001	Sensor source
BE5000	Bottom tracking error velocity maximum; set to 5 m/s
BA20	Bottom tracking evaluation amplitude minimum; set to 20 counts
BC200	Bottom tracking correlation magnitude minimum; set to 200 counts
BP001	Bottom tracking pings per ensemble; set to 1
BX5000	Bottom tracking maximum tracking depth; set to 500m

Table 2. Density and composition ratio of marine organisms sampled by Frame-type Midwater Trawl net at offshore Funka Bay

Net sampling frequency	Abundance of sampled zooplankton and nekton (ind./m ³)						Total
	euphausiids	copepods	amphipods	chaetognaths	gelatines	nekton	
Haul 1	89.65	0.15	1.53	3.53	0.00	0.00	94.86
	94.51 %	0.16 %	1.61 %	3.72 %	0.00 %	0.00 %	100 %
Haul 2	62.55	0.31	1.83	5.93	0.00	0.00	70.62
	65.94 %	0.33 %	1.93 %	6.25 %	0.00 %	0.00 %	100 %
Haul 3	86.61	0.78	3.22	12.77	0.39	0.00	103.77
	91.30 %	0.82 %	3.39 %	13.46 %	0.41 %	0.00 %	100 %
Haul 4	66.68	0.21	1.70	4.82	0.02	0.00	73.43
	70.29 %	0.22 %	1.79 %	5.08 %	0.02 %	0.00 %	100 %
Haul 5	63.15	0.80	1.30	3.46	0.03	0.00	68.74
	91.87 %	1.16 %	1.89 %	5.03 %	0.04 %	0.00 %	100 %

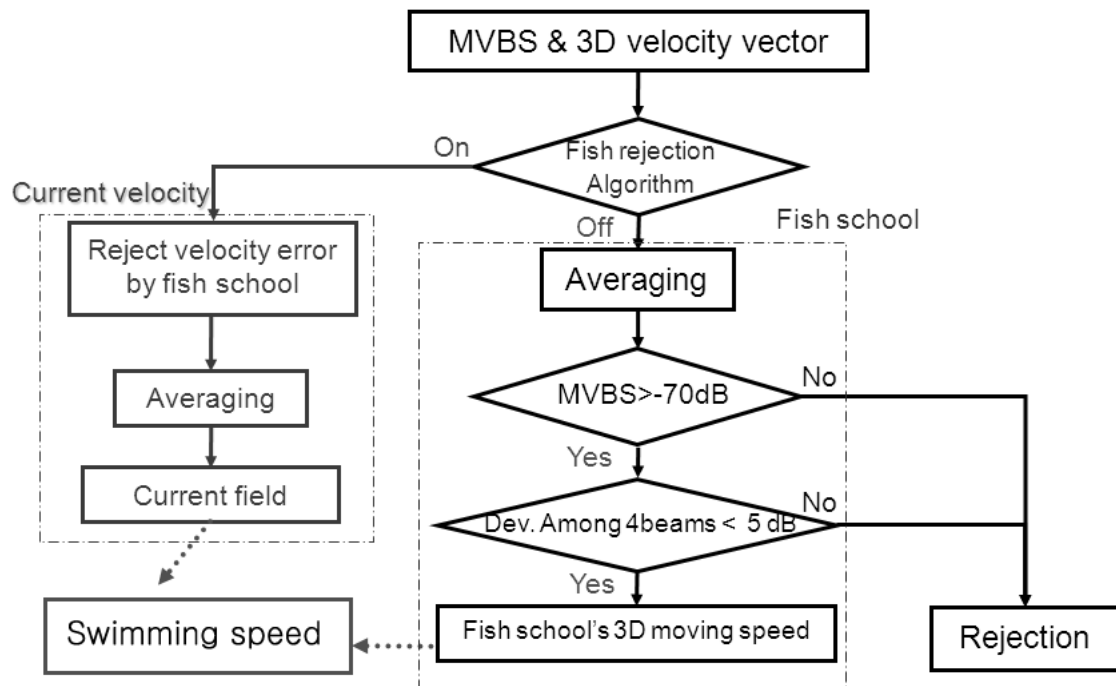


Fig. 1. Data processing to estimate the fish school's swimming speed by ADCP.

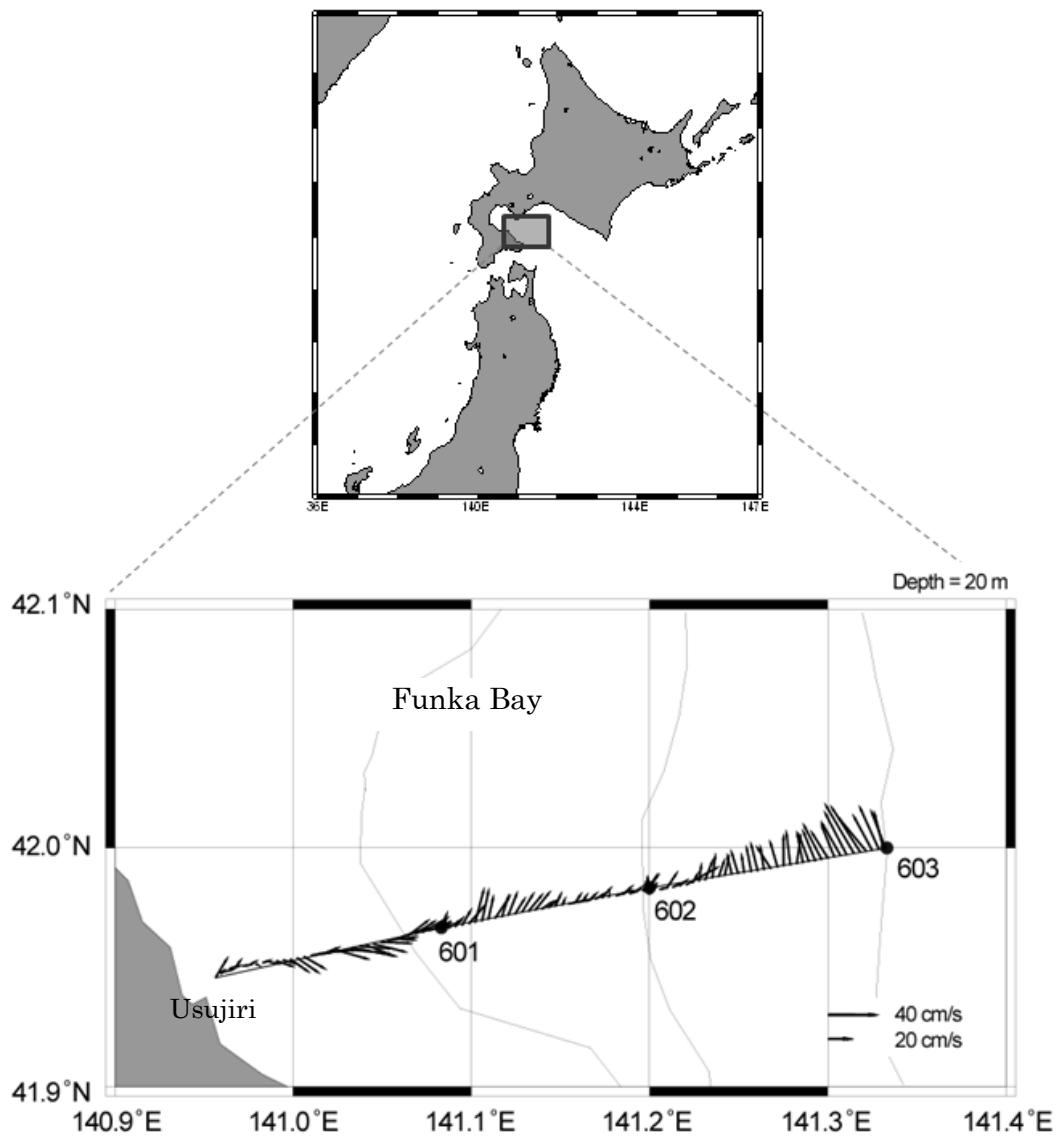


Fig. 2. Horizontal distribution current velocity along the track line of *T/S Ushio Maru* at a depth of 20 m measured by the shipboard ADCP offshore Funka Bay during September 27-28, 2003.

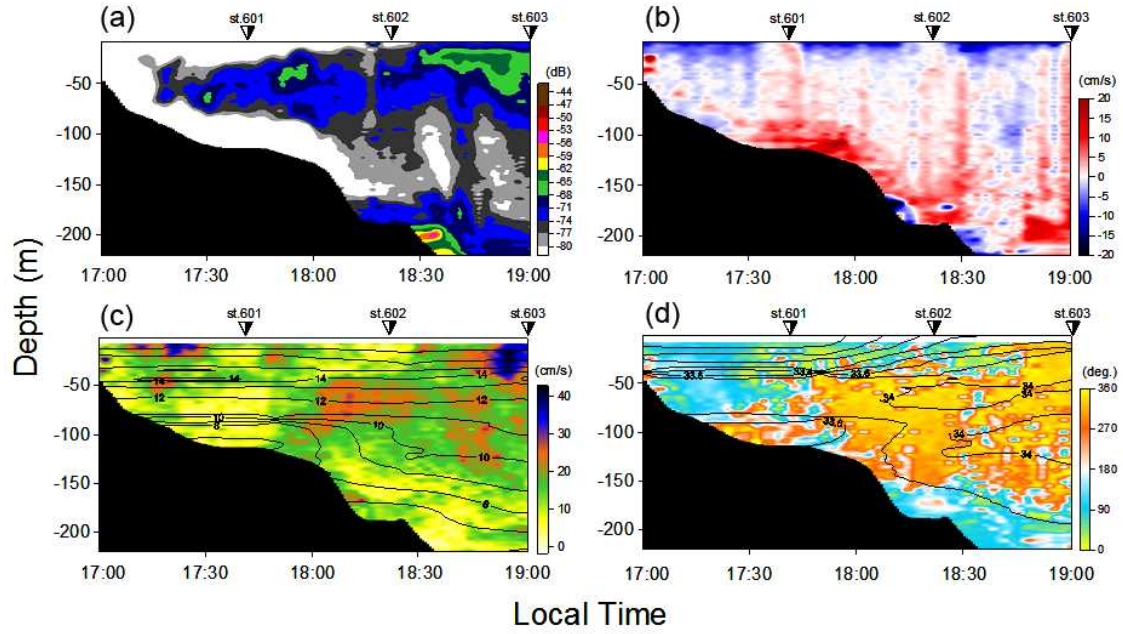


Fig. 3. Vertical distributions of MVBS, and current velocity along the track line of *T/S Ushio Maru* measured by the shipboard ADCP. MVBS was averaged for one minute (a), and the current velocity displayed for vertical velocity component (+ : upward, - : downward) (b), horizontal velocity (c) and direction (d), respectively. Contour lines of temperature (c) and salinity (d) are superimposed on the chart.

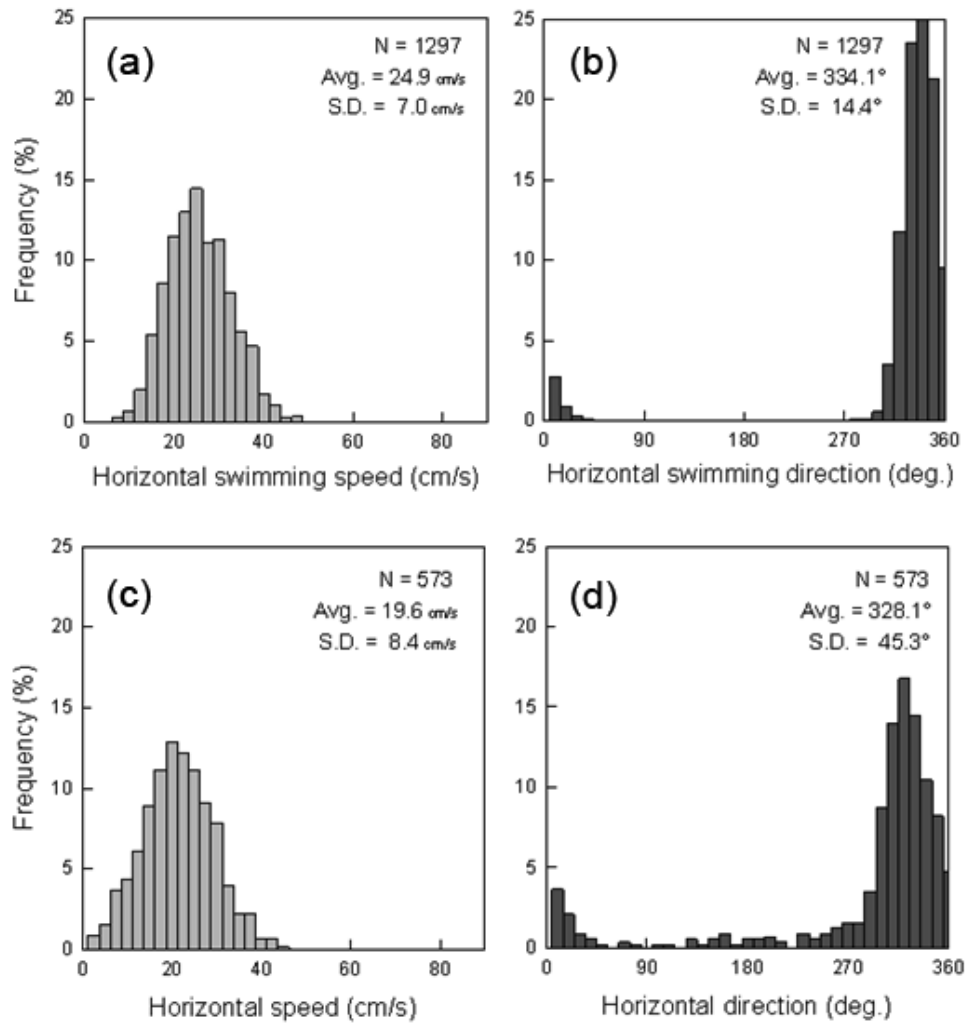


Fig. 4. Distribution of horizontal moving velocity of Sound Scattering Layer (a, b) and horizontal current velocity of surrounding waters (c, d). The SSL was identified by the threshold of MVBS (> -80 dB).

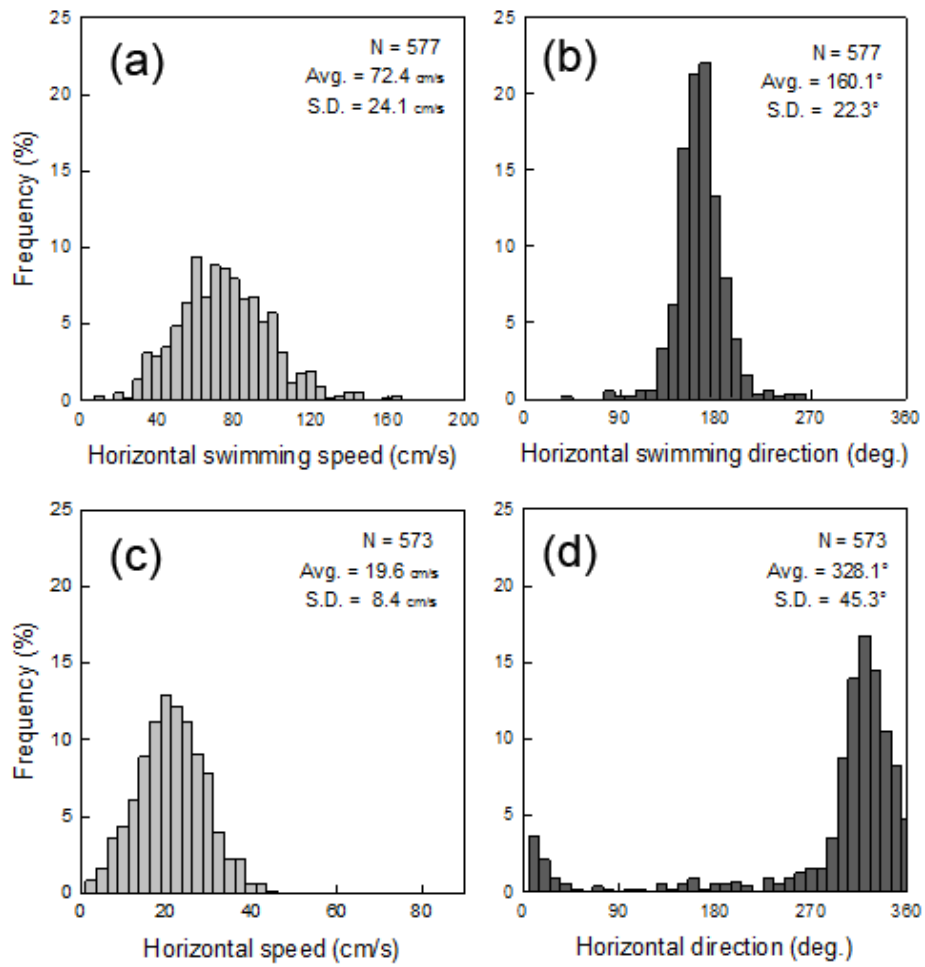


Fig. 5. Distribution of swimming speed (a) and direction (b) of fish school and current speed of waters (c, d) estimated by ADCP. The echo from fish school was identified by the threshold level of MVBS (>70 dB) and the noise margin less than 5 dB.

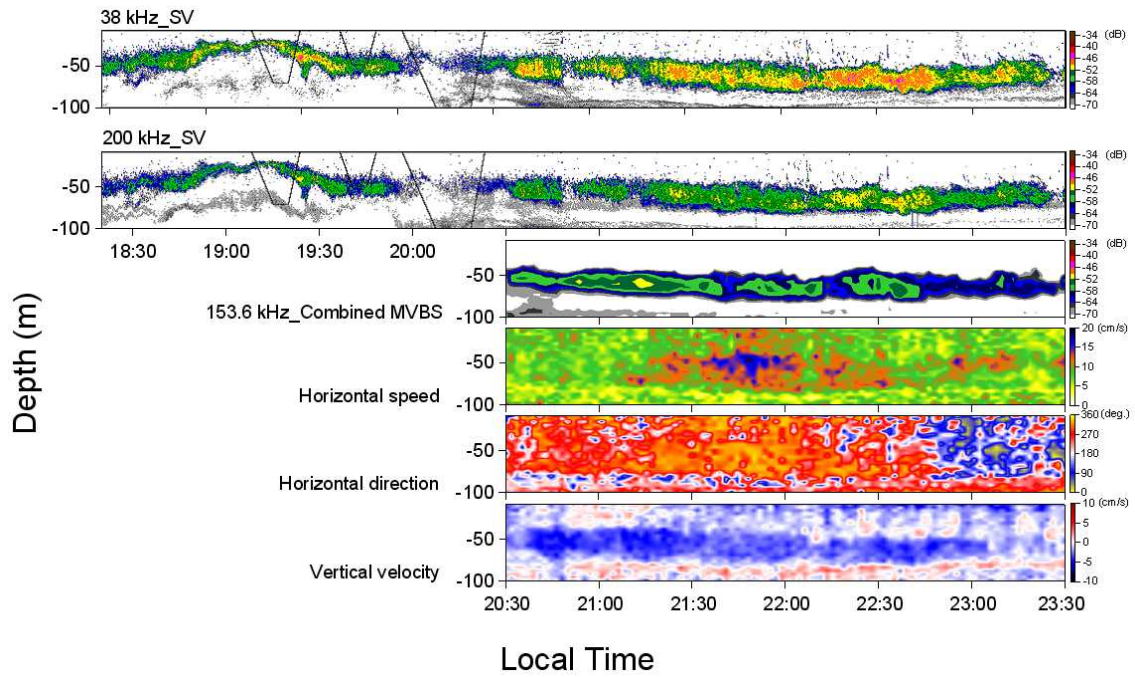


Fig. 6. Vertical distribution of MVBS and current velocity observed by scientific echo sounder and ADCP. The upper two echograms were obtained by 38 kHz and 200 kHz of EK60, and the lower four figures were obtained by MVBS, horizontal speed, horizontal direction, and vertical velocity from ADCP, respectively. Black line in the figure shows the track of Framed Midwater Trawl.

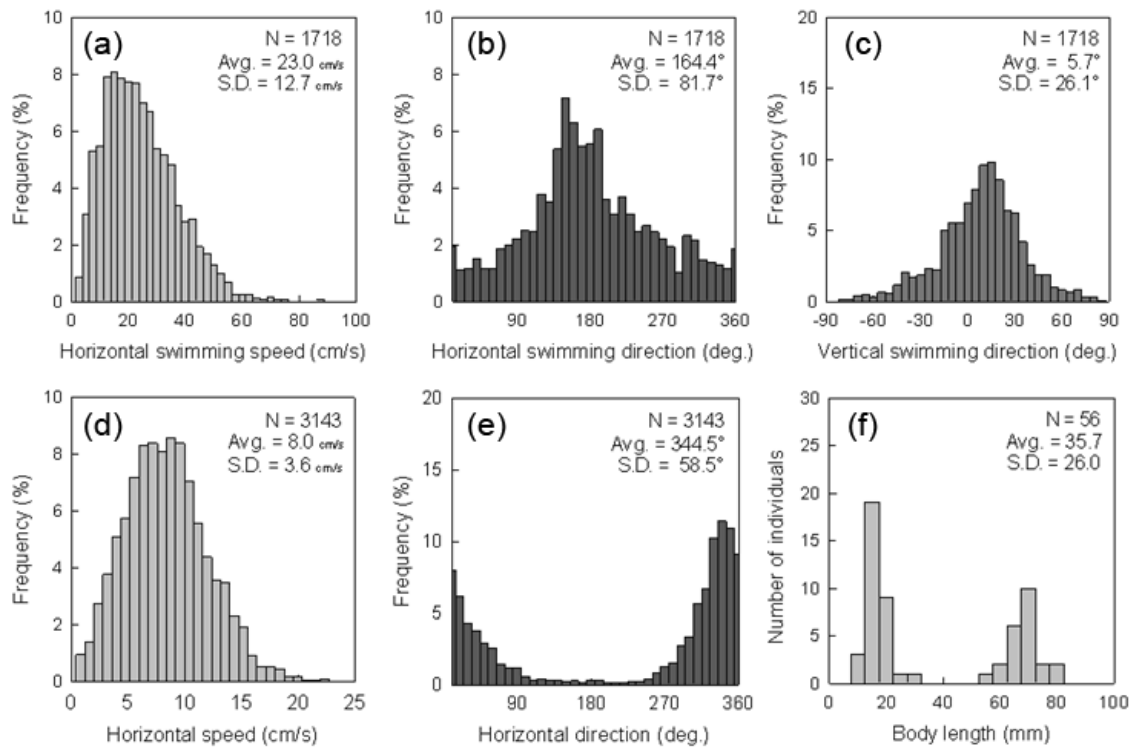


Fig. 7. Histograms of horizontal swimming speed (a), direction (b) and swimming angle (c) for lanternfish, and the current speed (d) and direction (e) of surrounding waters. Histogram of body length (f) of samples shows bimodal distribution. The large mode of body length was 66.2 mm (SD ; 6.1 mm).